LARGE TILT-ANGLE PHOTOTHERMAL OPTICAL BEAM STEERING USING MICROPATTERNED CNT-BASED INFRARED ABSORBER ON MULTILAYER THIN FILM STRUCTURES

Harris J. Hall[1], Sean A.McDaniel[1], Fahima Ouchen[1,2], Jose L. Figueroa[1,2], David Torres[1], Piyush J. Shah[1,3], Emily M. Heckman[1], and LaVern Starman[1]
[1]Air Force Research Laboratory, Wright-Patterson AFB, Ohio, USA
[2]KBR Inc., Dayton, Ohio, USA
[3]Apex Microdevices, West Chester, Ohio, USA

ABSTRACT

This work demonstrates photothermal actuation of asymmetrically patterned multi-layer thin film structures across a large range of mechanical tilt motion (up to 28° maximum). The device design constrains motion to 1D and is fabricated via post processing on a polysilicon foundry process. A key aspect is the micropatterning of an aerosol jet printed CNT coating as a stress free infrared absorber that enhances the response. Experimental results of the photothermal (λ=1532 nm) unit step response for both CNT coated and uncoated structures show linear tilt behavior up to ~ 50 W/cm^2 with CNT coated structures improving photosensitivity four fold. Beyond this irradiance level, the tilt magnitude responses suggests a mechanical bifurcation being triggered in the CNT coated structures. These results show significant potential for photo-actuated smart structures suitable for tunable optical beam steering applications.

KEYWORDS

Photothermal actuation, CNT, multi-layer, micro-optics; optical beam control, infrared absorber

INTRODUCTION

Light induced mechanical actuation has long been of interest for autonomous microsystems that require electrical isolation, often due to cost, complexity, or energy limitations. Some compelling examples manipulate the incident radiation itself by modulating the transmitted power ([1], [2]) or by altering the optical phase characteristics ([3], [4]). Our team has been interested in developing devices that when illuminated with a strong optical source can preferentially steer a portion of the incident radiation off-axis in a tunable fashion to large angles. This idea of “steering light with light” affords an unconventional self-powered smart structures approach to enable wireless optical beam scanning and steering.

We previously reported up to 9° of photothermally induced steady-state mechanical tilt at ~54 W/cm^2 irradiance with large deformation multilayer film structures that resemble the shape of a tetragonal pyramid [3]. These structures were constructed from selectively patterned regions of gold and silicon nitride films on polysilicon and exploit the residual stress inherent within these films to elevate the structure out of plane upon removal of the underlying sacrificial layer. This prior work added a 200 nm thick chromium film to one “side” of the pyramid to create asymmetric infrared (IR) absorption and subsequent tilting behavior upon illumination with an IR laser. However, these devices suffered from significant film delamination of the Cr layer, cross-coupled motion, and burn-in effects .

In this work, we address these deficiencies by modifying the structural design to better constrain the motion to one dimension (1D) tilt and by incorporating a patterned CNT-based film in place of the Cr as the infrared absorber. We show through experimental examination of the photothermal unit step behavior considerable improvement in dynamic range, photosensitivity, and directionality of the steady-state tilt response in comparison to prior work and offer some insight to the device dynamics.

Device Background

The devices characterized in this work are shown in Figure 1a-b and include a variant with and without the CNT infrared absorber in order to enable direct experimental comparison of photothermal actuation performance. The layout and geometry is identical to the structures previously examined in [3], expect these structures only have a single “arm” highly deformed out of plane upon removal of the sacrificial layer causing the central plate to be initially tilted 21° (see Figure 1c). As in prior work, the deformation of this arm is a result of the alternating tensile stress gold and compressively stressed silicon nitride films on the surface of the polysilicon structure which effectively creates a series of S-shaped deformation profiles that elevate that portion of the structure. Figures 2a-b. illustrate the film stack used in this arm for a single S-shaped cantilever with the addition of the CNT IR absorber on the surface. Device operation is almost entirely dependent on the photothermal response of this single raised arm whose internal thermal film stresses relax when heated, reducing deformation and subsequently the tilt angle of the central plate as illustrated in Figure 2c. The effect of the CNT coating is only considered on this single raised arm as the other three arms in the structure are not patterned with the compressive nitride layer.

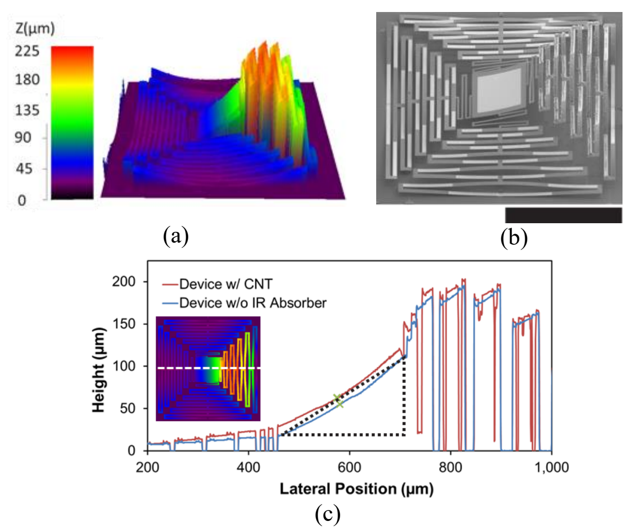

Figure 1: Post HF release characterization (a) 3D confocal microscope surface height image of Si_3N_4 on right arm only without IR absorber (b) SEM image of device with CNT absorber coating on the right arm. Scale bar is 500 µm in length. (c) 1D center cross-section of each device. Both structures have near equivalent tilt on 21° and cross axis tip of <1°, with a difference in piston height of ~8 µm.

These three other arms have little self-induced deformation and thus remain relatively fixed during operation effectively serving as support springs for the central reflective plate. This "single-arm" design reduces the structure's degrees of freedom essentially eliminating piston and cross axis tip motion upon actuation, making it advantageous for controlled 1D tilt motion.

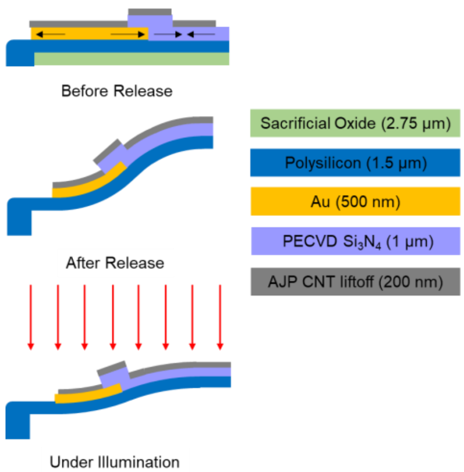

Figure 2: Simplified cross-section of a single multi-layer film cantilever with CNT coating. Note there is no effective stress in the CNT coating.

FABRICATION

The device fabrication process used the same core methods outlined in Refs [3,4] with the PECVD nitride layer (1µm thick) directly post-processed onto PolyMUMPS™ foundry produced die. Film thicknesses are summarized in Figure 2. The CNT coating was patterned through a combined use of aerosol jet printing (AJP) and liftoff processing (see Figures 1b, 3a-c). The AJP utilized a commercial ink (NINK-1100, NanoLab Inc.) and printed at room temperature using a 150 µm diameter nozzle. The CNT liftoff process used a standard AZ5214 photoresist (1.5 µm thick) and acetone spray gun, followed by rinses in isopropyl alcohol and deionized water. While the yield uniformity of the film was imperfect and discontinuous, the coverage was clearly sufficient for use as an IR absorber. The resulting contrast in CNT patterning was clearly superior when compared against our groups CNT film subtractive patterning attempts inspired by [5] (see Figure 3d).

Similar processing of AJP metals [6], oxides [7], and graphene oxide films [8], has been reported but to our knowledge this is the first demonstration liftoff with AJP CNTs. An important advantage of the CNT coating is that it has no significant film stress and thus minimal impact on the initial deformation (see Figure 1c). This decoupling of the infrared absorption from the structure greatly simplifies design.

EXPERIMENTAL SETUP

Both the steady-state and dynamic rise and fall photothermal step responses were examined experimentally using the setup illustrated in Figure 4a-b. A step excitation was applied using an infrared fiber laser (IPG photonics, λ = 1532 nm) focused across the width of the structure (spot size = 970 µm diameter) at increasing irradiance levels each for a 2 sec exposure time controlled using an automated beam block. The mechanical tilt (i.e. beam steering response) was measured by observing the reflection of a second low power visible laser (λ = 632 nm, spot size = 200

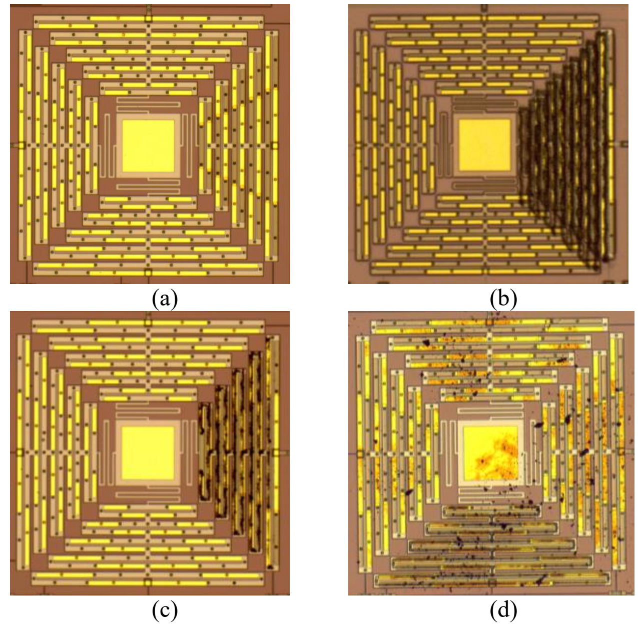

Figure 3: Patterning of CNTs as IR absorber (a) Si_3N_4 on right arm only w/o IR absorber pre-HF release (b) device after aerosol jet printing on patterned liftoff resist (c) same device after liftoff before HF release (d) attempted subtractive patterning 4-arm Si_3N_4 structure (as in [3]) with a CNT/nanodiamond/PMMA blend (inspired by [5]) on bottom arm

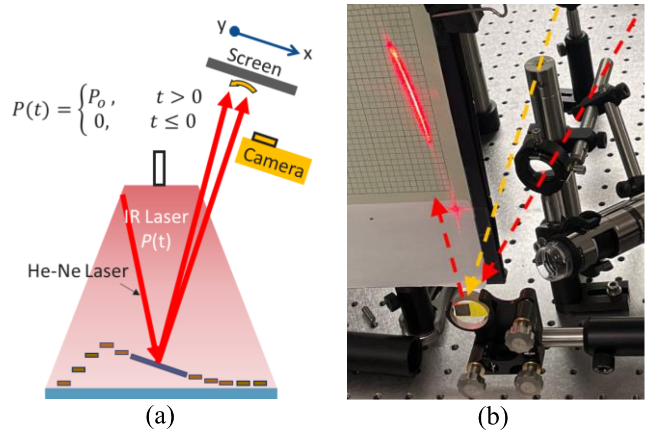

Figure 4: Experimental Setup (a) Graphical Illustration (b) Actual image of device under test and spot on screen. Red and orange dashed lines illustrate the visible and infrared beam paths respectively. The high speed camera imaging the screen is not shown.

µm diameter) off of the Au coated central plate onto a screen (distance = 11.1 cm) with a high speed camera (KronTech Chronos 1.4 - 6456 fps). Two separate test series were performed on each of the two devices, one with a CNT coating and one without. Each series increased the laser power and applied each condition twice to capture any burn-in effects and check for repeatability in the measurement. The "low power" series (see Figure 5) ramped the incident irradiance from 4.7 W/cm^2 to 68.8 W/cm^2 in increments of ~8-12 W/cm^2 while the "high power" series ramped from 48.4 W/cm^2 to 142.2 W/cm^2 in increments of ~11-30W/cm^2. The power increments had some variation due to inherent nonlinearities in the laser source power voltage control. All power levels were calibrated using a power meter in the plane of the device prior to the start of the experiment.

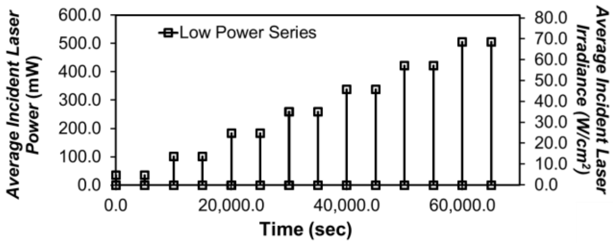

Figure 5. Low Power Unit Step Experimental Test Series. Camera is triggered for 3.25 sec capture with a 2 sec laser on time. High Power Series (not shown) is structured similar.

The raw video data sets collected were each post-processed using ImageJ and MATLAB to perform background removal and appropriately determine the center of mass (CoM) of the laser spot for each frame. The spot motion, from which optical tilt magnitude is measured, was converted from the CoM pixel position to angle based upon the geometry of the setup. The steady-state position for each point was determined by averaging the CoM of the central 100 frames (~ 1 sec after the step) during laser illumination . The rise and fall times were extracted from the 10% and 90% tilt magnitudes relative to initial and steady-state positions using 15th order polynomial fits to the rise and fall regions of each data set.

RESULTS AND DISCUSSION

As an example, the results for a single photothermal step response for the structure without the infrared absorber coating at an irradiance of ~ 45 W/cm^2 are shown in Figure 6a-e. In this instance the tilt motion of the structure is highly unidirectional and continuous in nature as desired.

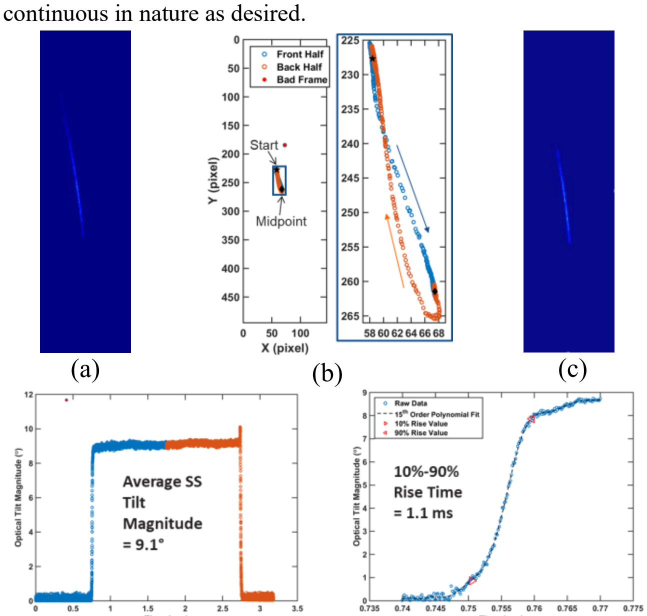

Figure 6: Portion of example unit step data set (w/o CNT 338 mW) at 6456 fps (a) Post-processed He-Ne laser spot screen image (artificially colored) at "Start" (unilluminated) (b) Laser spot CoM on screen, motion shown by colored arrows (c) Post-processed He-Ne laser spot screen image near "Midpoint" (illuminated) (d) Optical Tilt Magnitude time series relative to initial position (e) same series examining rise response. The fall response (not shown) is similar with a 1.1 ms fall time.

The compiled steady-state results from both low power and high power series for both the CNT coated and uncoated devices are shown in Figure 7a-b. The steady-state results are positive in multiple respects. First, the results show no evidence of device deterioration and negligible burn-in effects for both devices across the full range of optical power levels examined. Second, at moderate irradiance levels (~5-50 W/cm^2) the response trends are highly linear for both devices which is preferable for targeted design. Third, the CNT devices coated structures are 4x more photosensitive and have 3x larger tilt range than the uncoated structures within this linear operating region. And lastly the CNT coated device exhibits a larger than expected angular range (28° max mechanical tilt) that saturates > 60 W/cm^2. The maximum tilt magnitude is unexpected because it exceeds the initial mechanical tilt (21°) shown in Figure 1, which suggests the possibility of a structural nonlinearity being triggered at higher incident optical power that causes the central plate to have some tilt in the opposite direction as opposed to lying flat on the substrate.

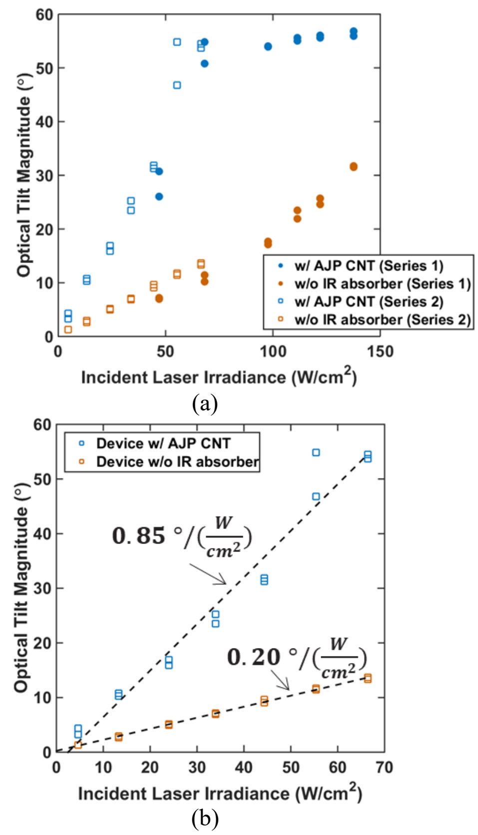

Figure 7: Steady-State Experimental Results (a) Compiled Optical Tilt Magnitudes for both High Power (Series 1) and Low Power (Series 2) Series (b) Low Power results with resulting photo sensitivities from linear least squares fitting.

A compilation of the dynamic 10%-90% rise time results for the low power series of both devices are shown in Figure 8a. The results clearly show a linear trend in these times with laser irradiance which is coincident with linear motion. Least squares fits to these plots show 4x the rise time sensitivity with respect to irradiance for the CNT coated devices vs. the uncoated devices which is coincident with the 4x increase in tilt photosensitivity. The data shows that the rise time is almost entirely dependent on the resultant tilt angle and independent of the CNT coating. For example, based upon the linear fits in Figures 7b and 8a, the irradiance required for 10° tilt is 14.2 W/cm^2 for the CNT coated device and 48.3 W/cm^2 for the uncoated, but the rise times are near equivalent at 1.16 ms and 1.20 ms respectively. The trends in 90%-10% fall times (not shown) are near equivalent. All rise and fall response times were measured to be less than 8 ms.

At higher irradiance levels (> 50 W/cm^2) the CNT coated structure exhibits a rapid jump in angular motion (Figure 8b) as evidenced by the gaps between sample points before reaching SS. The purple colored trace at 68.2 W/cm^2 shows the existence of an intermediate unstable mechanical state. This intermediate state is not always overserved when the test points are repeated. These results strongly suggest some form of a thermomechanical bifurcation is being triggered.

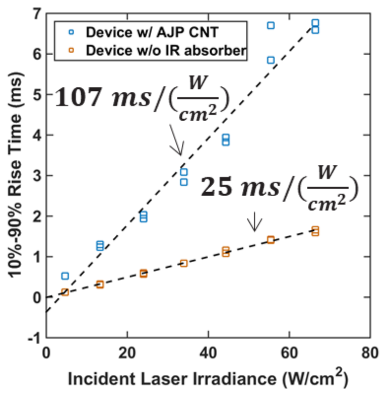

(a)

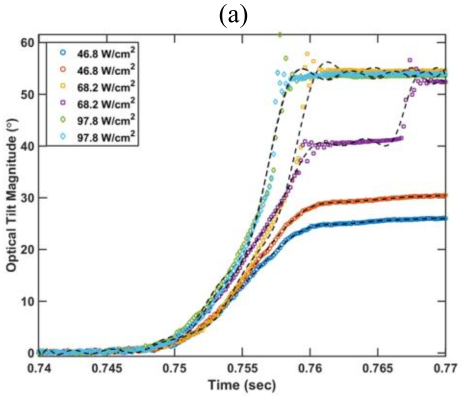

Figure 8: Dynamic Experimental Results (a) Compiled Optical Tilt Magnitude Rise Times for Low Power Series (b) Optical Tilt Magnitude Rise Behavior of CNT coated device near and above bifurcation threshold

CONCLUSIONS AND FUTURE WORK

The results of this work clearly demonstrate photothermal tilt control using the thermal stress relaxation mechanism of an asymmetrically constructed large deformation thin film structure for mechanical angles up to 28° in magnitude. The work also clearly demonstrates the utility of using AJP CNTs in conjunction with liftoff as a means for clean selective patterning of a stress-free infrared absorber on MEMS devices.

Future work is being directed towards incorporating geometric nonlinearity into our finite element simulations of the structures to enable predictive design (not shown) and towards expanding investigation into the structural bifurcation behavior observed. Lastly, improved blends of CNT feedstock for the AJP that can provide more uniformity across a broad range of surfaces are offered as a further area for improvement.

ACKNOWLEDGEMENTS

A portion of this work was supported under contract award FA807518D0015 by the Air Force Research Laboratory for on-site support by KBR Inc. The authors would like to thank Mr. Andrew Browning (AFRL) for plasma etching, Mr. Daniel Brooks (AFRL) for SEM imaging, and Mr. Juan Pastrana (Michigan State University) for helpful discussion.

REFERENCES

[1] X. Zhang, Z. Yu, C. Wang, D. Zarrouk, J.-W.T. Seo, J.C. Cheng, A.D. Buchan, K. Takei, Y. Zhao, J.W. Ager, et al. “Photoactuators and motors based on carbon nanotubes with selective chirality distributions.” *Nature Communications,* 5, 2983 (2014),

[2] H. Zeng, O.M. Wani, P. Wasylczyk, R. Kaczmarek, A. Priimagi, “A. Self-Regulating Iris Based on Light-Actuated Liquid Crystal Elastomer.” *Advanced Materials* 29, 1701814 (2017)

[3] H.J. Hall, S. McDaniel, P. Shah, D. Torres, J. Figueroa, L. Starman, “Photothermal Optical Beam Steering Using Large Deformation Multi-Layer Thin Film Structures. Micromachines”, 12, 428 (2021). doi:10.3390/mi12040428

[4] H.J. Hall, S. McDaniel, D. Torres, P. Shah, L. Starman, “Photothermal Frequency Response Characterization of Large Deformation Multi-layer Thin Film Structures.” In Proceedings of the 2020 IEEE Joint International Frequency Control Symposium— International Symposium on Applications of Ferroelectrics (IFCS-ISAF), Keystone, CO, USA, (2020)

[5] V.J. Gokhale, O. A. Shenderova, G. E. McGuire, M. Rais-Zadeh, “Infrared Absorption Properties of Carbon Nanotube/Nanodiamond Based Thin Film Coatings” *Journal of Microelectromechnical Systems*, 23, 1, (2014) doi: 10.1109/JMEMS.2013.2266411

[6] Y. Fu, Y. R. Liang, Y. Cheng and P. Wu, "A Combined Process of Liftoff and Printing for the Fabrication of Scalable Inkjet Printed Microstructures on a Flexible Substrate," in *IEEE Transactions on Electron Devices*, vol. 62, no. 4, pp. 1248-1254, (2015), doi: 10.1109/TED.2015.2401599.

[7] Y. Fu, J. Pan, K. Tsou and Y. Cheng, "A Flexible WO3-Based pH Sensor Array for 2-D pH Monitoring Using CPLoP Technique," in *IEEE Electron Device Letters*, vol. 39, no. 6, pp. 881-884, (2018), doi: 10.1109/LED.2018.2826013

[8] Y.-M. Fu, M.-C. Chou, C.-H. Kang, Y.-T. Cheng, P.-W. Wu, G.-Y. Chen, E. B. Secor, M. C. Hersam, "An Inkjet Printing Technique for Scalable Microfabrication of Graphene-Based Sensor Components", *Access IEEE*, vol. 8, pp. 79338-79346, (2020) doi: 10.1109/ACCESS.2020.2990501.

CONTACT

*H.J. Hall, tel: +1-937-713-8980; harris.hall.3@us.af.mil